[4]Srinivasan, G. R., Baeder, J. D., Obayashi, S., and McCroskey, W. J., "Flowfield of a Lifting Rotor in Hover: A Navier–Stokes Simulation," *AIAA Journal*, Vol. 30, No. 10, 1992, pp. 2371–2378.

[5]Roe, P. L., "Approximate Riemann Solvers, Parameter Vectors, and Difference Schemes," *Journal of Computational Physics*, Vol. 43, No. 2, 1981, pp. 357–372.

[6]Yoon, S., and Kwak, D., "Implicit Navier–Stokes Solver for Three-Dimensional Compressible Flows," *AIAA Journal*, Vol. 30, No. 11, 1992, pp. 2653–2659.

[7]Patankar, S. V., *Numerical Heat Transfer and Fluid Flow*, Hemisphere, New York, 1980, pp. 48, 49.

[8]Chen, C.-L., and McCroskey, W. J., "Numerical Simulation of Helicopter Multi-Bladed Rotor Flow," AIAA Paper 88-0046, Jan. 1988.

[9]Piziali, R. A., "2-D and 3-D Oscillating Wing Aerodynamics for a Range Angles of Attack Including Stall," NASA TM-4632, Sept. 1994.

[10]Lane, D. A., "UFAT—A Particle Tracer for Time-Dependent Flow Fields," *Proceedings of Visualization '94* (Washington, DC), IEEE Computer Society, 1994, pp. 257–264.

A. Plotkin
Associate Editor

Freestream Parameter Estimation Using Heat Flux Measurements

A. K. Alekseev*
RSC ENERGIA, Korolev,
Moscow Region 141070, Russia

Nomenclature

e	= specific energy, $C_v T$
f	= flow parameters (ρ, U, V, T)
P	= pressure
Q	= heat flux
Re	= Reynolds number
T	= temperature
t	= time
U	= velocity
X, Y	= coordinates
μ	= viscosity

Subscripts and Superscripts

comp	= computation
exp	= experiment
w	= wall conditions
∞	= freestream parameters

Introduction

WHEN it is necessary to determine flow parameters governing heat transfer, the need to solve inverse convection problems arises. For example, determining the boundary heat flux using temperature measurements at another boundary is discussed by Moutsoglou[1] for a two-dimensional region with steady-state flow described by the Navier–Stokes equations. Estimation of freestream parameters is of practical importance in many problems. Direct measurement of these parameters is accompanied by certain technical difficulties caused, for example, by flowfield distortion or the heat flux acting on the sensor. Wall temperature measurements are the simplest from this viewpoint.

The estimation of free flow parameters using heat flux measurements at different points at body surface is considered. Let us consider the supersonic gas flow described by equations of viscous compressible gas (Navier–Stokes). The set of freestream parameters governs heat flux distribution along the surface (along the X coordinate):

$$(\rho_\infty U_\infty T_\infty) \longrightarrow [Q_w(X_1),\ Q_w(X_2),\ Q_w(X_3)] \tag{1}$$

We seek to determine ρ_∞ U_∞ and T_∞ using heat flux measurements $Q_w(X_j)$ as the input data. We shall minimize the discrepancy between computed and experimental values of $Q_w(X_j)$, i.e.,

$$\varepsilon(\rho_\infty U_\infty T_\infty) = \sum_j \left[Q_w^{\exp}(X_j) - Q_w^{\text{comp}}(X_j) \right]^2 \tag{2}$$

The mathematical model consists of a flowfield solver and an optimization algorithm minimizing the discrepancy of computed and experimental data by varying the boundary conditions.

The Jacoby matrix $A_{ij} = \partial Q(X_i)/\partial f_j$ for the transformation $(\rho, T, U) \longrightarrow Q(X_1, X_2, X_3)$ is studied for the singularity search:

$$A_{ij} = \frac{\partial Q(X_i)}{\partial f_j} = \begin{bmatrix} \dfrac{\partial Q(X_1)}{\partial \rho} & \dfrac{\partial Q(X_1)}{\partial U} & \dfrac{\partial Q(X_1)}{\partial T} \\ \dfrac{\partial Q(X_2)}{\partial \rho} & \dfrac{\partial Q(X_2)}{\partial U} & \dfrac{\partial Q(X_2)}{\partial T} \\ \dfrac{\partial Q(X_3)}{\partial \rho} & \dfrac{\partial Q(X_3)}{\partial U} & \dfrac{\partial Q(X_3)}{\partial T} \end{bmatrix} \tag{3}$$

The determinant is identically equal to zero in the following events (global singularity). 1) The flowfield is determined not by the total parameter space $(\rho_\infty U_\infty T_\infty)$ but by some subspace of the lower dimension, for example, $(Re_\infty M_\infty)$. 2) The heat flux $Q_w(t, X)$ is determined not by total space of flow parameters but by some subspace of lower dimension. 3) The spatial heat flux variation $Q_w(X)$ is multiplicative along the X coordinate: $Q_w(X) = Q_w(X_0)F(X/X_0)$, i.e., the heat flux is self-similar along X.

The computation of the matrix A determinant allows one to consider the singularity only locally in regard to the flow parameters because of the problem nonlinearity. A global singularity can be detected by means of the Lie group. In particular, the transformation $Q(X) = Q(X_0, \rho_\infty U_\infty T_\infty)\varphi(X/X_0)$ corresponds to the Navier–Stokes equations invariance relative the operator $B = \eta(\rho_\infty U_\infty T_\infty)\partial/\partial X$. This operator is absent in the set of the Lie group basis of the Navier–Stokes equations that provides the absence of this type of singularity. Nevertheless, the transformation $Q(X) = Q(X_0, \rho_\infty U_\infty T_\infty)\varphi(X/X_0)$ can take the place for an infinitely thin boundary layer. Thus, although the matrix (3) is nonsingular, it can be very close to a singular one that causes instability.

A global singularity exists for special events and can be easily detected by computations. The most practical interesting problem arises when a global singularity is absent. In that event, the nonlinearity of the problem becomes crucial. $Q_w(t, X)$ nonlinearly depends on $(\rho_\infty U_\infty T_\infty)$ and nonlinearly varies along X. Then, there is a six parameter local transformation: $(X^3 \times f^3) \times f^3 \longrightarrow Q^3$. If this transformation is smooth and if f^3 and Q^3 are smooth manifolds, then, according to the Sard theorem,[2] such a transformation should be nonsingular (in the common case). If $\det[\partial Q(X_i)/\partial f_j]$ is not identical to zero, the set of points $X \in R^3$ for which $\det[\partial Q(X_i)/\partial f_j] = 0$ is either empty or a smooth two-dimensional surface embedded into R^3 space. It can be easily seen that f^3 and Q^3 are smooth manifolds, and the transformation is smooth for flows considered here (having no shocks on the surface). Thus, the problem [Eq. (1)] will be nonsingular with the probability close to 1.

These speculations lead to the conclusion that, if the numerical experiments have demonstrated nonsingularity in some point, the problem is nonsingular in a significant part of the phase space.

A number of difficulties arise at the investigation of the Navier–Stokes problem, in general, which are connected with the need for repeated solution of the direct problem and large computation time. In this connection, the two-dimensional spatially evolutional flows that can be solved with quick marching methods are of special interest. The supersonic flow over a flat plate with a compression corner was considered. The flowfield was computed using the parabolized Navier–Stokes (PNS) method. The finite difference method with second-order accuracy in the Y direction (symmetrical differences with fourth-order smoothing) and first order in X was used. At every

Received May 14, 1996; revision received March 31, 1997; accepted for publication April 3, 1997.

*Senior Researcher, Department of Aerodynamics and Heat Transfer.

Table 1 Comparison of different condition criteria

Problem	$\det_2(A)$	$\det_3(A)$	$\mathrm{Cond}_2(A)$	$\mathrm{Cond}_3(A)$	$\det_2(M)$	$\det_3(M)$	$\mathrm{Cond}_3(M)$
a	11.0	0.448	2.5	111	167	0.2	3859
b	2.0	0.35	10	143	3054	3637	1800

new step along the marching coordinate, flow parameters are determined via time relaxation:

$$\frac{\partial \rho}{\partial t} + \frac{\partial(\rho U)}{\partial X} + \frac{\partial(\rho V)}{\partial Y} = 0 \tag{4}$$

$$\frac{\partial U}{\partial t} + U\frac{\partial U}{\partial X} + V\frac{\partial U}{\partial Y} + \frac{1}{\rho}\frac{\partial P}{\partial X} = \frac{1}{\rho}\frac{\partial}{\partial Y}\mu\frac{\partial U}{\partial Y} \tag{5}$$

$$\frac{\partial V}{\partial t} + U\frac{\partial V}{\partial X} + V\frac{\partial V}{\partial Y} + \frac{1}{\rho}\frac{\partial P}{\partial Y} = \frac{4}{3\rho}\frac{\partial}{\partial Y}\mu\frac{\partial U}{\partial Y} \tag{6}$$

$$\frac{\partial e}{\partial t} + U\frac{\partial e}{\partial X} + V\frac{\partial e}{\partial Y} + \frac{P}{\rho}\left(\frac{\partial U}{\partial X} + \frac{\partial V}{\partial Y}\right) = \frac{1}{\rho}\left[\frac{\partial}{\partial Y}\lambda\frac{\partial T}{\partial Y} + \frac{4}{3}\mu\left(\frac{\partial U}{\partial Y}\right)^2\right] \tag{7}$$

where $P = \rho RT$ and $e = C_v T$.

The mass, momentum, and energy conservation laws are described by Eqs. (4–7). The external flow is assumed to be spatially uniform. The undisturbed flow is set on the entry boundary and the external one: $T_\infty(t)$, $\rho_\infty(t)$, $U(y, 0) = U_\infty(t)$, and $V(y, 0) = 0$. On the plate surface, we have the adhesion $V = U = 0$ and wall temperature $T_w(X)$. The heating rate is determined from the temperature gradient at the wall. The program was verified at the boundary layer and the oblique shock separate computation with acceptable results. The computation field contains up to 100 nodes in the cross direction and from 250 to 900 steps in the evolution direction. The time of one direct computation was about 2–5 min of PC/486.

The sensitivity matrix A_{ij} [Eq. (3)] and some its functions were calculated for estimation of problem rank: 1) $\det(A)$, determinant; 2) $\mathrm{cond}(A)$, conditionality[$\mathrm{cond}(A) = \lambda_{\max}\lambda_{\min}^{-1}$]; and 3) $\det(M)$, determinant and spectrum of eigenvalues λ_i of Fisher's informational matrix ($M_{jm} = A_{ij}\,A_{im}$).

The number of $\nu_i = (|\lambda_i|)^{0.5}$ exceeding input data dispersion determines the number of parameters that can be retrieved, i.e., the local rank of the problem. This rank was determined during testing of the PNS solver. Approaching the boundary layer the self-similar solution ν_1 remain constant (order of 10^2), but ν_2 and ν_3 decrease to values of about 10^{-3}. The problem became less conditioned as the measurement points converge and the Mach number increases. These calculations confirm the validity of problem rank estimation by PNS. It is obvious that as $M \to \infty$ ($U_\infty \to \infty$) the influence of T_∞ on heat transfer decreases and the problem becomes more ill conditioned.

The values of conditionality are presented in Table 1 for two problems that follow: problem a, flat plate measurements in a laminar regime applied to Ref. 3 data ($M_\infty = 14.1$, $Re_\infty = 10^5$, and $T_\infty = 72$ K); and problem b, flat plate and compression corner (15 deg) measurements in a laminar regime (without separation account) applied to Ref. 3 data. Subscripts 2 and 3 correspond to the number of parameters (M_∞ Re_∞) or (M_∞ Re_∞ T_∞). Eigenvalues of informational matrix are, for the plate (problem a), $\lambda_1 = 38.0$, $\lambda_2 = 0.37$, and $\lambda_3 = 0.01$; and for the compression corner (problem b), $\lambda_1 = 326.0$, $\lambda_2 = 18.5$, and $\lambda_3 = 0.26$.

Numerical Experiments

In numerical experiments the flow parameters (ρ_∞ U_∞ T_∞) were determined using the heat flux $Q(X)$ variation along the wall that was obtained in computations. The optimization problem was solved by a type of the method of Nelder–Mead.[4] The numerical experiments confirmed the feasibility of freestream parameters estimation using heat flux measurements.

The problem [Eq. (1)] has rank 1 for an isothermal wall in the boundary-layer approach. Within the PNS framework, the problem has rank 3 but it is poorly conditioned. The flow self-similarity along the evolutional coordinate is absent in the PNS approach due to the finite boundary-layer thickness. We hope that the nonlinearity of the flow parameters transformation to the heat flux and not self-similar heat flux transformation along the evolutional coordinate (excluding multiplicative transformation) should provide nonsingularity of the problem. The flow parameters determination for this problem investigation at rank values 2–3 was performed for experimental data of Ref. 3. This flow is not self-similar but the influence of T_∞ is weak due to high M numbers. The set of two to three parameters (M, Re, T) or (ρ, U, T) was determined using $Q_w(X)$ values at three points on the flat plate. The flow parameters estimation results are provided in Table 2 with heat flux fitting accuracy about 8%.

Table 2 Results of flow parameters estimation

M_∞	Re_∞	T_∞K	Value
14.1	10^5	72	Experimental
14.5	8.7×10^4	—	Computed (two parameters, plate)
14.4	6.6×10^4	50	Computed (three parameters, plate)
13.3	1.2×10^4	65	Computed, three parameters (compression corner)

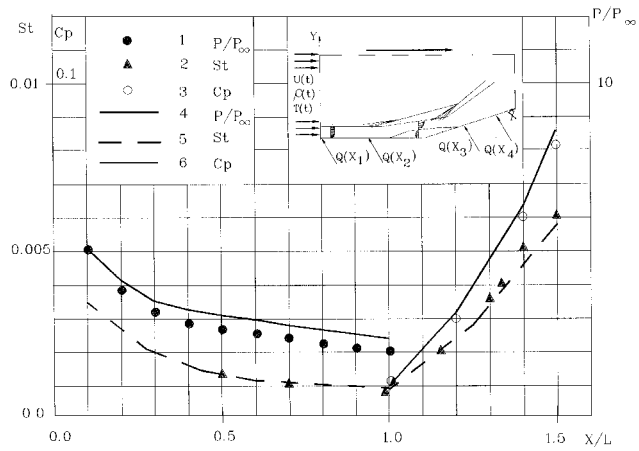

Fig. 1 Comparison of computed data vs experiments[3] for compression corner (15 deg): 1, experimental P/P_∞; 2, experimental St; 3, experimental $Cp = P/\rho_\infty U_\infty^2$; 4, computed P/P_∞; 5, computed St; and 6, computed $Cp = P/\rho_\infty U_\infty^2$.

The accuracy of the results decreases at the estimation of three parameters. The results have a stochastic character (depending on the initial guess, we get different values).

The analysis of problems conditionality (Table 1) demonstrates that problem b is most conditioned. The quality of the matching to the experimental data of Ref. 3 is shown in Fig. 1. The corresponding flow parameters are presented in Table 2.

Discussion

Most present work on inverse convection problems concerns boundary geometry determination using a preassigned flowfield or minimization of some functional (drag or heat flux, for example). Other classes of inverse convection problems are poorly studied at present despite a practical need for them and the progress being made in computers. This is for a number of reasons. The practical interesting convection problems usually are two to three dimensional in space and are time dependent, which demands multidimensional input data with a large number of parameters. Usually, we do not have information about all of the flow parameters but only about some nonlinear functions of these parameters.

The nonlinear function of the flow parameters $Q_w(X)$ retains information on the parameters ρ_∞ U_∞ and T_∞ in a transformed form. The rank value is of special interest for transformation:

$$(\rho_\infty\, U_\infty\, T_\infty) \to [Q_w(X_1),\ Q_w(X_2),\ Q_w(X_3)]$$

For various flow classes, this rank can be 1, 2, or 3. Even if the rank is 3, the problem can be very close to a singular one. $Q_w(X)$ nonlinearly depends on $(\rho_\infty U_\infty T_\infty)$ and nonlinearly varies along X. The qualitative analysis shows that it would be appropriate to measure heat flux at points with maximum different flow type. The corresponding quantitative criteria are the determinant and the conditionality of the sensitivity matrix A_{ij} and the spectrum of eigenvalues λ_i of Fisher's informational matrix ($M_{jm} = A_{ij} A_{im}$). The numerical experiments and experimental data show that the problem condition can be improved by the location of the measurements in zones of different flow type (at the plate and the edge, for example). Therefore, the measurement points can be chosen before experiment by the optimization of the determinant or the conditionality.

The results of the Ref. 3 experimental data treatment confirm the feasibility of $\rho_\infty U_\infty$ and T_∞ determination using laminar heat fluxes. The estimation of two parameters for a flat plate and three parameters for a corner is feasible.

References

[1]Moutsoglou, A., "Solution of an Elliptic Inverse Convection Problem Using Whole Domain Regularization Technique," *Journal of Thermophysics*, Vol. 4, No. 3, 1990, pp. 341–349.

[2]Sternberg, S., *Lectures on Differential Geometry*, Prentice–Hall, Englewood Cliffs, NJ, 1964, p. 210.

[3]Lawrence, S. L., Tannehill, J. C., and Chaussee, D. S., "Application of Implicit MacCormack Scheme to the Parabolized Navier–Stokes Equations," *AIAA Journal*, Vol. 22, No. 12, 1984, pp. 1755–1763.

[4]Nelder, I., and Mead, R., "A Simplex Method for Function Minimization," *Computer Journal*, Vol. 7, No. 3, 1965, pp. 308–313.

J. Kallinderis
Associate Editor

Limiting Mach Number for Quantitative Pressure-Sensitive Paint Measurements

Donald R. Mendoza*
University of California, Berkeley, Berkeley, California 94702

Introduction

THE pressure-sensitive paint (PSP) technique for measuring surface pressure and obtaining coefficient of pressure (C_P) data has recently gained acceptance as an alternative and complement to traditional instrumentation systems and computational techniques. The PSP technique is based on the pressure sensitivity of photoluminescent materials and in its simplest form may be represented by an equation relating a reference wind-off to wind-on photoluminescence intensity

$$I_0/I = A + B(P/P_0) \tag{1}$$

where I is the PSP's photoluminescent signal, P is the surface pressure, A and B are the PSP Stern–Volmer sensitivity coefficients, and the subscript refers to a reference level. The fundamentals and several applications of PSP measurements based on Eq. (1) are introduced by Morris et al.[1] and reviewed by McLachlan and Bell.[2] A detailed development of the PSP governing equations, including Eq. (1), and a comprehensive uncertainty analysis of the PSP instrumentation system are presented in Mendoza.[3] This last study calculated uncertainty ($\mathrm{d}C_P$) of PSP derived C_P data by dividing PSP instrumentation system error sources into three categories including the PSP methodology, PSP implementation, and PSP imaging system. The random and bias error components corresponding to these categories were obtained by using representative noise values characteristic of first generation (typical) and state-of-the-art PSP instrumentations systems. [Typical systems are those where PSP photoluminescence is not corrected for significant influencing parameters other than pressure (e.g., temperature, photodecomposition, and excitation fluctuations) with a nonscientific grade imager, and where geometrical and optical inconsistencies between wind-on and wind-off images used in Eq. (1) are not corrected for.[3] With state-of-the-art systems, PSP photoluminescence is not significantly influenced by parameters other than pressure or is corrected for them, with a scientific grade imager (e.g., 14-bit A/D, low read out noise and low dark current, high capacity quantum wells), and the geometrical and optical inconsistencies between wind-on and wind-off images used in Eq. (1) corrected for.[3]] These errors were propagated into C_P calculations using a linearized Taylor series, as outlined in Bevington and Robinson,[4] with the additional assumption that error sources were independent such that all cross correlation terms in the series were zero. Final $\mathrm{d}C_P$ values were calculated using the rss uncertainty model corresponding to a 95% coverage level when the component bias and random errors are added by the rms method. These $\mathrm{d}C_P$ results were presented as a function of freestream Mach number (M_∞) and C_P. Additionally, these results identified critical sources of noise that must be addressed to minimize PSP measurement uncertainty.

Mendoza's analysis reemphasized the conclusion presented by Sajben[5] that PSP instrumentation systems were better suited for moderate to high Mach number flows. Mendoza showed that the primary reason for this was that $\mathrm{d}C_P$ scales approximately as one over the Mach number squared, manifesting into large errors in calculated C_P at low Mach numbers. Sajben's analysis was constrained to ideal test conditions such as uniform model surface temperature and the assumption that photodegradation of the PSP coating does not occur; Mendoza's was not. However, neither analysis determined the limiting M_∞ for obtaining quantitative PSP measurements with respect to traditional instrumentation systems (force balances and pressure taps).

This analysis develops a technique to determine the limiting M_∞ for acquiring quantitative PSP measurements of pressure. The analysis is based on defining C_P uncertainties in terms of coefficient of lift (c_l) uncertainties ($\mathrm{d}c_l$). The $\mathrm{d}C_P$ for quantitative PSP measurements will then be equated to the $\mathrm{d}c_l$ representative of quantitative measurements from traditional instrumentation systems. This approach is taken for the following four reasons. First, results from PSP measurements are presented in terms of C_P. Second, because C_P is a local surface parameter, its uncertainty varies at each point on a surface. Third, acceptable uncertainties of traditional measurement systems are usually quoted in terms of c_l. Fourth, because c_l is a global parameter, its uncertainty is a single value. Thus, in line with convention and convenience, the uncertainty in PSP C_P results will be related to an equivalent uncertainty in c_l. This transformation will be used in conjunction with $\mathrm{d}C_P$ vs M_∞ results from Mendoza's uncertainty analysis[3] to determine the limiting M_∞ for quantitative PSP measurements.

Analysis

The coefficient of lift may be obtained from surface pressure data as

$$c_l = \frac{1}{c}\int_0^c \Delta C_p \,\mathrm{d}x \tag{2}$$

where c is the chord length and ΔC_P is the difference between upper and lower surface coefficients of pressure. Using the first-order process for uncertainty propagation[4] as just described, the uncertainty in c_l due to the uncertainty in C_P may be obtained as

$$\mathrm{d}c_l = \frac{\partial c_l}{\partial \Delta C_P}\mathrm{d}\Delta C_P \tag{3}$$

The evaluation of the terms of Eq. (3) is as follows:

$$\frac{\partial c_l}{\partial \Delta C_P} = \frac{1}{c}\frac{\partial\left(\int_0^c \Delta C_P \,\mathrm{d}x\right)}{\partial \Delta C_P} = \frac{1}{c}\int_0^c \frac{\partial \Delta C_P \,\mathrm{d}x}{\partial \Delta C_P} = 1 \tag{4}$$

Received Oct. 28, 1996; revision received March 21, 1997; accepted for publication March 24, 1997.

*Ph.D. Candidate, Department of Mechanical Engineering; currently Postdoctoral Research Associate, National Research Council, NASA Ames Research Center, Mail Stop 227-2, Moffett Field, CA 94035-1000. Member AIAA.